Tree Physiology, 2026, **46**, tpaf166
https://doi.org/10.1093/treephys/tpaf166
Advance access publication date 26 December 2025
Research paper

Triple-isotope evidence for distinct physiological strategies of larch and cembra pine across the Holocene

Tito Arosio[1,*], Marco M. Lehmann[1], Markus Leuenberger[2,3] and Matthias Saurer[1]

[1]Swiss Federal Institute for Forest, Snow and Landscape (WSL), Zürcherstrasse 111, 8903 Birmensdorf, Switzerland
[2]Climate and Environmental Physics, Physics Institute, University of Bern, Sidlerstrasse 5, 3012 Bern, Switzerland
[3]Oeschger Centre for Climate Change Research, University of Bern, Hochschulstrasse 4, 3012 Bern, Switzerland

*Corresponding author (tito.arosio@wsl.ch)

Handling Editor: Daniel Epron

Stable isotopes of carbon, oxygen and hydrogen in tree rings provide a record of plant physiological processes and environmental variability. Although an increasing number of studies now apply triple-isotope approaches, no investigation has yet tested their temporal stability over millennial timescales or assessed the relative impacts of physiology versus climate on long-term isotopic signals. Here, we used 9000 years of multi-isotope records from co-occurring deciduous larch (*Larix decidua*) and evergreen cembra pine (*Pinus cembra*) at the Alpine treeline. We found a high interspecies coherence for $\delta^{18}O$ throughout the Holocene with a robust summer hydroclimate sensitivity, confirming its dominance by environmental drivers. In contrast, $\delta^{13}C$ and $\delta^{2}H$ show weaker and less stable coherence, reflecting species-specific physiology. Larch exhibits tight $\delta^{2}H$–$\delta^{18}O$ and $\delta^{2}H$–$\delta^{13}C$ correlations and stronger climate sensitivity, consistent with its reliance on freshly assimilated carbon. Pine, by contrast, shows weaker $\delta^{2}H$–climate relationships and frequent decoupling from $\delta^{13}C$ and $\delta^{18}O$, reflecting potential storage use and metabolic fractionations. Thus, inter-isotope relationships reveal that $\delta^{18}O$ is a robust long-term climate proxy, while $\delta^{13}C$ and $\delta^{2}H$ encode contrasting carbon-use strategies and metabolic processes across species that may vary over time. Together, these findings demonstrate that multi-isotope, multi-species approaches not only strengthen climate reconstructions but also provide a physiological dimension to long-term isotope records.

Keywords: conifer, *Larix*, *Pinus*, stable isotopes, treeline.

Introduction

Stable isotope ratios in tree-ring cellulose are important proxies for studying both past climates and plant physiology (McCarroll and Loader 2004, Siegwolf et al. 2022, Gessler et al. 2024, Huang et al. 2024). The oxygen isotope ratio ($\delta^{18}O$) in tree rings primarily reflects the isotopic signature of source water (precipitation) and the degree of evapotranspiration enrichment (Roden and Farquhar 2012, Treydte et al. 2014). It is a robust proxy for hydroclimate because leaf water is enriched in ^{18}O as transpiration progresses before being transferred to cellulose (Barbour 2007, Saurer et al. 2012). $\delta^{18}O$ exhibits a strong coherence with climate variables such as drought, making it especially valuable for paleoclimate reconstructions on regional to continental scales (Büntgen et al. 2021, Yang et al. 2021, Nagavciuc et al. 2022, Treydte et al. 2024, 2006, Liu et al. 2025).

Carbon isotope ratio ($\delta^{13}C$) in tree rings is linked to leaf gas exchange processes and is an indicator of intrinsic water-use efficiency (iWUE) and stomatal regulation (Craig 1954, Farquhar and Sharkey 1982). The primary driver of $\delta^{13}C$ variability is the ratio of intercellular (ci) to atmospheric (ca) CO_2 concentrations (ci/ca), which determines carbon isotope discrimination during carboxylation in the Calvin cycle (Farquhar and Sharkey 1982, Farquhar et al. 1989). This ci/ca ratio is dynamically regulated by the balance between net photosynthetic CO_2 assimilation (A_{net}) and stomatal conductance (g_s), and is closely linked to intrinsic water-use efficiency (iWUE = A_{net}/g_s) (Tcherkez et al. 2011). Thus, $\delta^{13}C$ in cellulose records how trees optimize carbon gain versus water loss, serving as an integrated measure of drought response and physiological performance (Farquhar et al. 1989, Saurer et al. 1995).

The hydrogen isotope ratio ($\delta^{2}H$) in tree-ring cellulose has been less explored, but it may offer novel insights into plant physiological processes (Cormier et al. 2018, Vitali et al. 2022, Lehmann et al. 2024*b*), particularly after the recent methodological advances that improved the reliability of its analysis (Leuenberger and Filot 2007, Loader et al. 2015, Saurer et al. 2025) which measure the carbon-bound hydrogen, as the oxygen-bound hydrogen is exchanged with laboratory water during sample measurement (Filot et al. 2006). The carbon-bound hydrogen comes from xylem source water and also from organic metabolites (via exchange with NADPH and other hydrogen carriers during cellulose biosynthesis) (Cormier et al. 2018). The $\delta^{2}H$ values in cellulose are also influenced by the isotope effects on metabolic pathways decoupling, which can be large, up to $>100‰$ in different tree species (Holloway-Phillips et al. 2024, Lehmann et al. 2024*b*). As a result, $\delta^{2}H$ in tree rings encodes a mix of environmental and metabolic information (Vitali et al. 2023, 2022), including modifications of carbon metabolism in response to stress conditions (Lehmann et al. 2021). Disturbances like insect defoliation or severe drought can force trees to rely on stored sugars, imprinting a metabolic $\delta^{2}H$ signal that diverges

Received: June 30, 2025. **Accepted:** December 14, 2025

from the normal climate-driven pattern, leading to a δ^2H decoupling from $\delta^{13}C$ and $\delta^{18}O$ (Vitali et al. 2023, Charlet De Sauvage et al. 2025, Neycken et al. 2025).

So far, dendroclimatology studies have mainly used single-isotope approaches, particularly using $\delta^{13}C$ or $\delta^{18}O$, and yielded high-quality hydro-climate reconstructions from centennial to multi millennial timescales (Helama et al. 2018, Yang et al. 2021). However, the combined use of multiple isotopes, each reflecting complementary aspects of tree physiology, has the potential to yield novel insights. For example, $\delta^{13}C$ and $\delta^{18}O$ together disentangled the relative roles of stomatal conductance and carbon assimilation (Siegwolf et al. 2023): a parallel increase of both would indicate stomatal limitation under drought stress, while a decoupled response may point to shifts in photosynthetic capacity (Siegwolf et al. 2023). The dual-isotope approach improved our understanding of plant carbon-water interactions (Scheidegger et al. 2000) and tree mortality reasons (Gessler et al. 2018). More broadly, the integration of $\delta^{13}C$, $\delta^{18}O$ and δ^2H may allow to separate environmental signal from physiological feedbacks (Loader et al. 2008) or improving the climate signal (Sidorova et al. 2008, Büntgen et al. 2021). It can detect when climatic signals are modulated by downstream metabolism, such as the decoupling of $\delta^{18}O$ and δ^2H under conditions of stress or altered carbohydrate allocation (Vitali et al. 2023, Lehmann et al. 2024a). Notably, the relationship between $\delta^{13}C$ and δ^2H remains the least explored (Neycken et al. 2025), although recent agricultural studies on wheat suggested positive associations between them (Sanchez-Bragado et al. 2019).

In the tree-ring isotope research the role of interspecies differences remains poorly studied since most isotope studies focus on single species, but many multi millennial paleoclimate studies combine data from co-occurring species to reach the needed sample depth (Friedrich et al. 2004, Nicolussi et al. 2009, Edvardsson et al. 2016). This overlooks potential biases arising from species-specific physiological responses. Addressing species effects is therefore essential for the reliable interpretation of long-term isotope records. Species differences in $\delta^{13}C$ and $\delta^{18}O$ have been documented in both conifers and broadleaves (Martínez-Sancho et al. 2023, Qi et al. 2024, Rezzouk et al. 2025). Species-specific isotopic values (δ^2H, $\delta^{13}C$) have been documented, yet the short-term covariance patterns remain consistently similar across species (Hartl-Meier et al. 2015, Arosio et al. 2020). However, long-term variations have not been thoroughly investigated.

Despite the growing number of tree-ring isotope records, only few studies have systematically explored how $\delta^{13}C$, $\delta^{18}O$ and δ^2H co-vary through deep time and across species. However, species-specific differences in carbohydrate dynamics and water-use strategies may bias the climatic signal captured by each isotope. This is particularly critical for hydrogen, where metabolic effects may override environmental signals.

Here, we analyze the Alpine Holocene Triple Tree Ring Isotope Record (AHTTRIR) (Arosio et al. 2022) from larch (*Larix decidua*) and cembra pine (*Pinus cembra*) trees that grew at the treeline in the Central Alps database. It uses this unique dataset of cellulose $\delta^{13}C$, $\delta^{18}O$ and δ^2H spanning from 2015 to ca 9000 BP. This allows us to address several aims:

(i) Inter-species coherence—we compare isotope records from larch and cembra pine to disentangle common climate signals from species-specific physiological imprints. By evaluating the temporal stability of inter-species coherence over 9000 years, we assess how consistently shared or divergent signals are expressed through time.

(ii) Climate sensitivity of each isotope—we quantify how $\delta^{13}C$, $\delta^{18}O$ and δ^2H in each species correlate with environmental variables (e.g., moisture, temperature, drought indices, 1900–2015) and investigate the stability and coherence of inter-isotope relationships, as a measure of how consistently climate signals are expressed across physiological pathways.

(iii) Mechanistic insights and multi-proxy integration—we explore the physiological mechanisms underlying observed isotope relationships, including the coupling between carbon and water cycles (carbon–water coupling) in the trees. We discuss how processes like stomatal control, photosynthetic acclimation and carbohydrate storage/use manifest in the multi-isotope patterns, and what this implies for interpreting long-term tree-ring records in terms of tree function and climate response.

Materials and methods

Samples and sampling sites

Holocene wood remains (n = 186) and wood material from modern, i.e., living trees (n = 16) were collected at the alpine treeline environment. Samples include the 86 evergreen cembra pine (*Pinus cembra*) and 114 deciduous european larch (*Larix decidua*), gathered a SW–NE transect in the central European Alps (46°02′–47°03′ N, 7°00′–12°15′ E) from 29 different sites, spanning elevations from 1930 to 2400 m a.s.l. Holocene wood sections were available at the Department of Geography of the University of Innsbruck, where the Eastern Alpine Conifer Chronology (EACC) has been established on the basis of calendar-dated tree-ring-width series (Nicolussi et al. 2009). Cores from living trees of the two species were taken in 2015 at three treeline sites in the Swiss Alps with up to five trees sampled per species at breast height, avoiding compression wood. The combined dataset of modern and subfossil wood samples spans from 6980 BCE (8880 BP) to 2015 CE with a 5-year temporal resolution and the data are in the publicly available AHTTRIR (Arosio et al. 2022). This is based on a measurement of 7708 isotope ratios of $\delta^{18}O$, δ^2H and $\delta^{13}C$.

Tree ring width and dating

Tree-ring widths (TRW) were measured with a precision of 0.001 mm using a LINTAB device and TSAPW software. Mean TRW series were established by cross-dating and averaging radii. In case of pith decay, the number of missing inner rings was estimated (pith-offset, PO) to determine cambial age of a sample. Modern samples were dated using known sampling dates, while relict samples were cross-dated with reference chronologies through statistical and visual controls (Nicolussi et al. 2009).

Cellulose extraction and triple stable isotope analysis

The triple isotope analyses of carbon, oxygen and hydrogen isotope ratios ($\delta^{13}C$, $\delta^{18}O$, δ^2H) were carried out using wood blocks of consecutive five tree rings at the level of individual trees. The separation of wood samples into 5-year blocks was performed at the University of Innsbruck, Austria. The choice

of 5-year blocks was a compromise between time resolution and total number of manageable samples. For cellulose extraction, wood samples were cut into wedges and 5-year tree-ring blocks were prepared without pooling between trees and then scaled to 20–50 mg dry weight, accounting for the expected weight loss during α-cellulose extraction. The blocks were subsequently cut into slices (<1 mm), packed in heat-sealed fiber filter bags and individually labeled.

Alpha cellulose extraction followed a modified Jayme-Wise procedure (Borella et al. 1999, Boettger et al. 2007). Samples were delignified in 1% $NaClO_2$ + CH_3COOH solution at 70 °C for 30+ h, then treated with 17% NaOH at 25 °C for 45 min. After neutralizing with 1% HCl, samples were washed until pH ~7 and dried at 50 °C, with drying time dependent on sample size (Ziehmer et al. 2018).

The triple-isotope analysis followed protocols previously established by Loader et al. (2015). For simultaneous measurements of $\delta^{13}C$, $\delta^{18}O$ and $\delta^{2}H$ values, cellulose samples underwent high-temperature pyrolysis (>1450 °C) in a Flash HT elemental analyzer, converting the cellulose into carbon monoxide and hydrogen gasses according to the methodology described by Filot et al. (2006). This high temperature is crucial for decomposing the cellulose quantitatively into hydrogen and carbon monoxide, with the residue (partial carbon of the cellulose) (Leuenberger and Filot 2007) collected in a graphite crucible. The resulting gasses were separated via a 5 Å molecular sieve and analyzed using a Thermo Delta XP or an Elementar/Isoprime mass spectrometer for $\delta^{13}C$ and $\delta^{18}O$ on CO and $\delta^{2}H$ on H_2. The fraction of exchange and the carbon-bound non-exchangeable $\delta^{2}H$ values are subsequently calculated following the equations in Filot et al. (2006). The specific procedure involves equilibrating the cellulose samples with waters of known $\delta^{2}H$ values (−429.1‰) at 110 °C for 10 min using a continuous flow of helium carrier gas at 80 mL min^{-1}. The samples and standards are stored in a desiccator when not being analyzed. This equilibration method was cross-calibrated with a nitration method to determine the $\delta^{2}H$ values of cellulose (Filot et al. 2006). Calibration and quality control were integral to our methodology. A two-point calibration of the raw delta values obtained against our working gas was performed for all isotope ratios. For hydrogen, we used Merck cellulose and IAEA-CH7 polyethylene standards. This calibration approach allows us to determine the offset and contraction/stretching of the scale relative to the international VSMOW-SLAP scale. These scale correction terms are independent of whether there are available exchangeable hydrogen atoms. To check for drift in the reference gas and to evaluate precision over time, we additionally used Wei Ming 101 cellulose (from WEI MING Pharmaceutical MFG) and/or IAEA-C3 cellulose (form IAEA) and IAEA-C6 sucrose (form IAEA) standards (Rozanski et al. 1992, Coplen 1994). This led to the evaluation of the machine performance and the implementation of the necessary corrections to a linear drift. Furthermore, the inclusion of IAEA-CH7 specifically enabled quality control of the non-exchangeable hydrogen measurements (i.e., no exchangeable portion), while the cellulose standards accounted for the exchangeable portion. The system's stability allowed for consistent and reliable data within the standard precision limits of ±0.3‰ for oxygen, ±0.15‰ for carbon and ± 3.0‰ for hydrogen (Loader et al. 2015).

For all the $\delta^{13}C$ values after 1000 CE we applied the factor described in Leuenberger (2007) to correct for the $\delta^{13}C$ depletion of CO_2 caused by the Industrial Revolution from about 1850 onwards (Leuenberger 2007).

Age trend correction and larch hydrogen correction

As tree-ring isotope data can exhibit species-specific juvenile age-related trends (Arosio et al. 2020), we applied the 80-year spline Regional Curve Standardization (RCS) method separately for each species and for each isotope (Briffa et al. 1996) (Figure S1 available as Supplementary Data at *Tree Physiology* Online). This approach removes age-related trends while preserving low-frequency variability and maintaining the absolute values of the original time series (Esper et al. 2003, Helama et al. 2018). Specifically, for each species, we calculated cambial age for each ring and fit a smoothing spline to the mean isotope values grouped by age. For rings younger than a species-specific age threshold (e.g., 130 years for $\delta^{18}O$ and $\delta^{13}C$, 400 years for $\delta^{2}H$), we subtracted the spline value from the raw isotope data to obtain detrended values, minimizing ontogenetic effects while retaining the climate signal. For older rings, no correction was applied to preserve potential long-term trends. The hydrogen values are known to be lower in larch than non-larch trees (Arosio et al. 2020). Thus, we corrected all larch values based on the average difference between the larch and non-larch species in the Alpine database. The correction factor is −48.1‰ (Arosio et al. 2024).

Inter-species and inter-isotope correlation

Correlations between isotopes were assessed for at the tree and species level. Pearson correlation coefficients (r) with corresponding *P*-values were calculated to quantify the relationships among isotopes within species. To evaluate the temporal evolution of isotope correlations, we calculated correlation coefficients for each individual tree and plotted them across their respective time spans, highlighting statistically significant values ($P < 0.05$). To assess the temporal dynamics of isotope relationships, we computed running Pearson correlations between $\delta^{13}C$, $\delta^{18}O$ and $\delta^{2}H$ using a centered moving window approach. Detrend Isotope time series were first normalized by individual sample, and averaged by year and species (Figure S2 available as Supplementary Data at *Tree Physiology* Online). Correlations were calculated using a rolling window of fixed length (50, 250, 500 and 1000 years), implemented via the zoo package in R (Zeileis et al. 2014). Analyses were performed separately for each species to evaluate differences in temporal coherence between isotope pairs. To understand the mutual temporal covariance between the two species in their rolling correlations, we calculated the correlation between the respective running correlation time series.

Climate sensitivity analyses

To assess the relationship between the isotope chronologies and climate, we first produced a mean chronology based on age-detrended data. Climate data for the period 1901–2010 CE were obtained from the Climate Explorer platform (https://climexp.knmi.nl/) for the grid 46.03–47.05°N, 7.55–12.25°E, which encompasses all sampling sites. Monthly records of precipitation, temperature, vapor pressure and Palmer drought severity index (PDSI) were extracted from the CRU TS 4.07 dataset (Harris et al. 2020). To match the temporal resolution of the isotope data, all climate variables were averaged into 5-year means.

We performed monthly climate sensitivity analyses over the full period (1901–2010 CE) by calculating Pearson correlation coefficients between the isotope chronology and each climate variable. The same analysis was repeated using first-differenced data to remove low-frequency trends in both the isotope and climate series (Figure S3 available as Supplementary Data at *Tree Physiology* Online). In addition, we conducted the analysis on subset data from the upper Engadin (Val Roseg VVR) site, where both species are present on the same site, using climate data extracted for the coordinates 46.26°N, 9.50°E (Figure S4 available as Supplementary Data at *Tree Physiology* Online). To test whether combining isotopes could enhance climate sensitivity, we additionally calculated a composite index by summing the z-scored δ^2H and δ^{18}O values at the individual-tree level before averaging across trees and species (Figure S5 available as Supplementary Data at *Tree Physiology* Online). For each isotope and grouping (larch, cembra pine, total), we assembled and calculated the mean Expressed Population Signal (EPS) and mean interseries correlation (Rbar) for the period 1900–2010, the period where the climate calculations are performed (Table S1 available as Supplementary Data at *Tree Physiology* Online).

Results

Interspecies isotope relationships

The chronologies of δ^{18}O, δ^2H and δ^{13}C values (Figure 1) exhibit varying degrees of agreement between the two species. The δ^{18}O values showed the strongest species coherence, indicated by a significant correlation between the δ^{18}O values of larch and cembra pine across the investigated 9000-year period (r = 0.50, $P < 0.001$; Figure 1a). This interspecies correlation is confirmed within the 1800–2000 CE period covered by living trees, is higher during 1800–1900 (r = 0.74, $P < 0.001$), and becomes less significant during 1900–2000 (r = 0.46, $P = 0.0323$; Figure 1b). Despite increased sample replication during the 1800–2010 period (Figure 1h), compared with the all span of the dataset (Figure 1g), the inter-species correlation shows no significant improvement compared with the complete database (Figure 1b). In contrast, δ^2H and δ^{13}C values do not show significant correlation between the species across the entire study period (larch: r = 0.06, $P = 0.014$; Figure 1c, cembra pine: r = −0.07, $P = 0.0069$; Figure 1e). During 1800–1900, δ^2H values show low correlation between species (r = 0.11, $P = 0.657$), but this correlation strengthens in the 20th century (r = 0.40, $P = 0.0682$; Figure 1d). Similarly, δ^{13}C values exhibit no significant correlation in the 19th century (r = −0.11, $P = 0.663$), yet a moderate positive correlation emerges after 1900 (r = 0.37, $P = 0.0898$; Figure 1f). The correlation values for both δ^2H and δ^{13}C increase with the greater sample replication (Figure 1h) during 1900–2010, though they remain statistically non-significant. In summary, the data show a strong species coherence in δ^{18}O values between larch and cembra pine, and a minimal one for δ^2H and δ^{13}C. The increased sample replication in the 20th century influences the δ^2H and δ^{13}C correlations, but not the δ^{18}O one. Chronology strength varies across isotopes. δ^{18}O shows the highest common signal, with interseries correlations of Rbar = 0.62 in larch and Rbar = 0.42 in cembra pine, yielding EPS values of 0.93 and 0.85, respectively; the pooled chronology reaches EPS = 0.91. δ^{13}C expresses a moderate signal (Rbar = 0.43, EPS = 0.86 in larch; Rbar = 0.30, EPS = 0.77 in cembra pine; pooled EPS = 0.86) (Table S1 available as Supplementary Data at *Tree Physiology* Online). δ^2H shows the weakest agreement Rbar = 0.28, EPS = 0.79 in larch; Rbar = 0.33, EPS = 0.75 in cembra pine; pooled EPS = 0.82) (Table S1 available as Supplementary Data at *Tree Physiology* Online). Using mean-depth EPS as the primary metric, δ^{18}O approaches adequacy, δ^{13}C is marginal and δ^2H falls below the conventional EPS ≈ 0.85 threshold.

Inter-isotope relationships and their temporal dynamics

Larch, but not cembra pine, shows a tendency toward positive correlations among the isotopes (Figure 2d–f). Among the three isotope pairings, δ^{13}C–δ^{18}O exhibits the strongest and most coherent relationship, evident at both the individual tree level (Figure 2c and f) and in its temporal evolution (Figure 3b). By contrast, δ^2H–δ^{18}O correlations are positive in larch but highly variable, including negative values, in cembra pine (Figures 2a, d and 3a). The δ^2H–δ^{13}C correlations also diverge, being significant in larch but weak or absent in cembra pine (Figures 2b, e and 3b). In larch, the correlations are generally positive and temporally stable, while in cembra pine δ^2H–δ^{18}O correlations are more variable, being both positive and negative with limited coherence across individual trees (Figure 3). The relationship between δ^{13}C and δ^2H is weak and inconsistent in cembra pine, with frequent shifts in sign and low significance. In contrast, some larch trees show more consistency, with moderate positive δ^2H–δ^{13}C correlations through time (Figure 3).

Running correlations among δ^2H, δ^{18}O and δ^{13}C chronologies are strongly influenced by the window length and indicate distinct temporal variability and species-specific differences across time (Figure 4). The δ^2H–δ^{18}O correlations are generally positive in both species, and larch consistently exhibits higher correlation, particularly at larger window sizes, consistent with the results above. At the 1000-year scale, δ^2H–δ^{18}O correlations in larch remain around $r = 0.5$ over large parts of the time series, whereas those of cembra pine are more variable and substantially weaker during the mid-Holocene. In shorter windows, both species show higher-frequency fluctuations, but species differences remain evident.

The δ^2H–δ^{13}C correlations of larch are weak, generally positive and strengthen with increasing window size, while those of cembra pine are more negative or near-zero, particularly between 6000 and 2000 BP. This divergence is most pronounced at the 1000-year scale, where opposing trends between species emerge. In contrast, δ^{18}O–δ^{13}C correlations show similar trajectories in both species, with a long-term trend toward increasingly negative correlations beginning around 5000 BP. This convergence becomes especially evident with the 1000-year window, suggesting a shared large-scale shift in the coupling between δ^{18}O and δ^{13}C. Together, these results indicate that δ^2H is the primary driver of interspecies divergence in multi-isotope relationships, while δ^{18}O remains the most coherent across species. Cross-species coherence of the running correlations depends on window length (Figure 4). For δ^2H–δ^{18}O, larch vs pine agreement is negligible: n.s. at 50 years; r = −0.09 (250), −0.07 (500), 0.08 (1000). δ^2H–δ^{13}C is similarly weak: n.s. at 50–500 years; r = 0.14 (1000). In contrast, δ^{18}O–δ^{13}C converges with scale: n.s. at 50 years; r = 0.28 (250), 0.64 (500), 0.77 (1000). Thus,

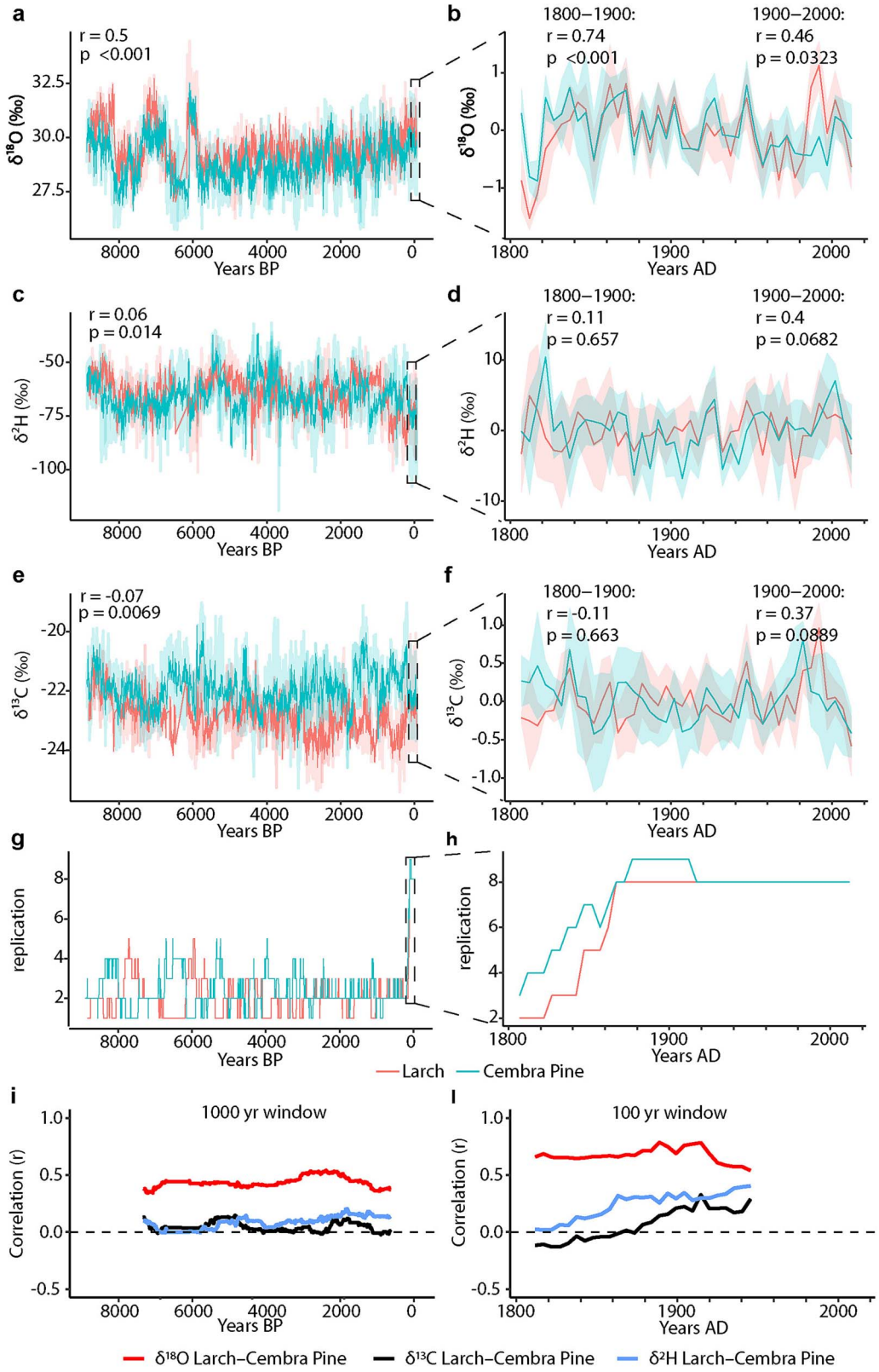

Figure 1. Temporal interspecies comparison of triple isotope chronologies of larch and cembra pine. Time series and interspecies comparisons of oxygen ($\delta^{18}O$; a, b), hydrogen ($\delta^{2}H$, c, d), and carbon ($\delta^{13}C$, e, f) isotopic compositions of tree-ring cellulose over the past 9000 years and the period 1800–2000 CE. Solid lines represent mean values and shaded areas denote inter-annual variability. For comparability, $\delta^{2}H$-values of larch have been corrected to align with cembra pine. Long-term series (a, c, e) are plotted against the BP timescale and include Pearson correlation coefficients (r) and associated *P*-values quantifying the agreement between species. The high-resolution subsets (b, d, f) focus on the last two centuries, split into pre-1900 and post-1900 intervals, with correlations assessed separately for each period. Replication of tree-ring samples over time for each species, g: full Holocene; h: 1800–2000 CE. Panels (i, l) illustrate the running Pearson correlations between larch and cembra pine isotope chronologies: (i) long-term correlations computed with a 1000-year moving window over the past 9000 years and (l) correlations over the period 1800–2000 CE based on a 100-year window. Colored lines denote the temporal evolution of correlations for each isotope pair ($\delta^{18}O$: red, $\delta^{2}H$: blue, $\delta^{13}C$: black), with the dashed line marking zero correlation.

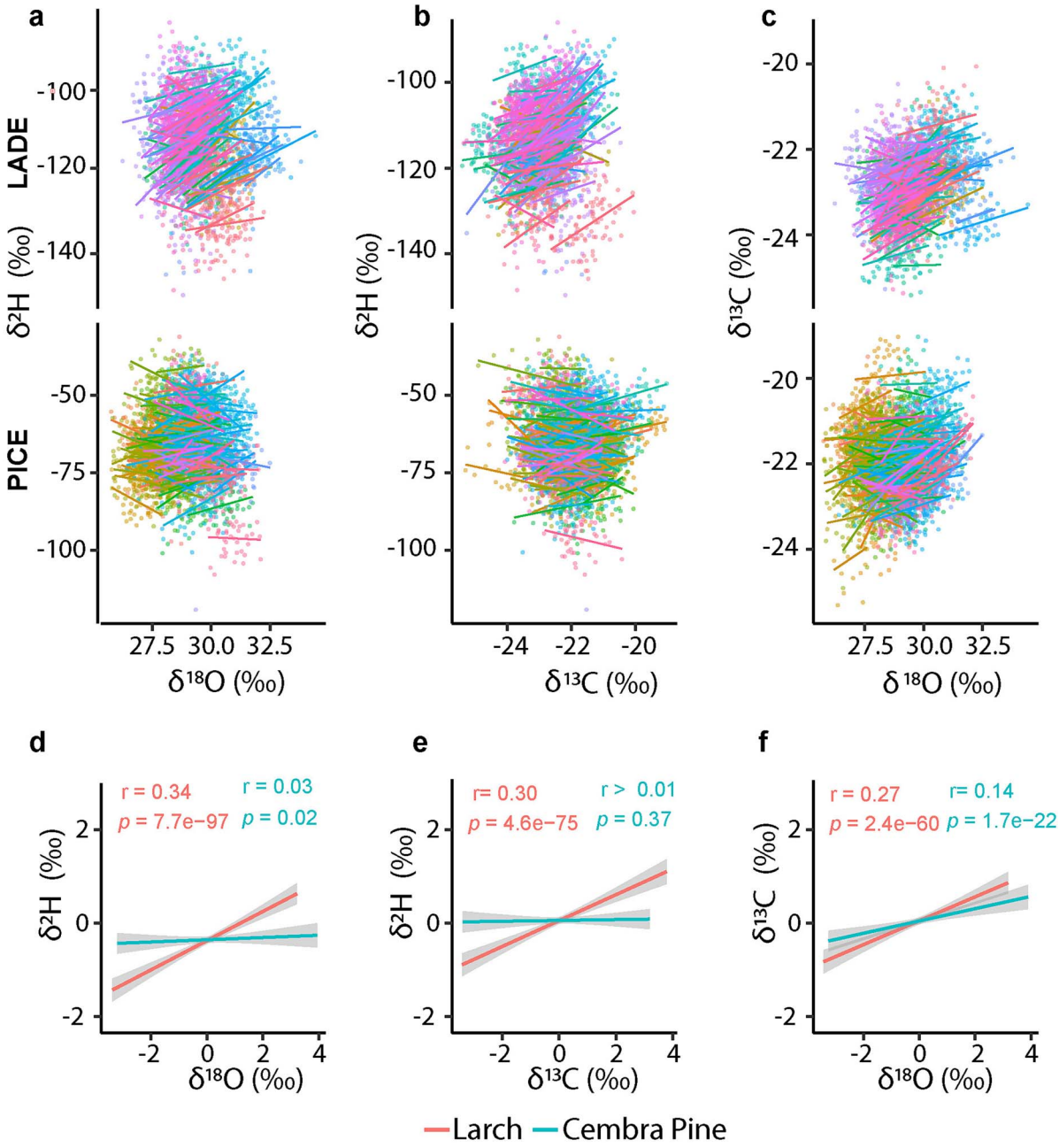

Figure 2. Triple isotope relationships for larch (LADE) and cembra pine (PICE). The data include the hydrogen (δ^2H), oxygen (δ^{18}O) and carbon (δ^{13}C) isotopic composition of tree-ring cellulose over the last 9000 years. The upper row (a, b, c) shows isotopic relationships for individual trees. Data points and linear regression lines are color-coded by trees. The lower row (d, e, f) shows the same relationships but across all trees of each species. Here the isotope data have been normalized. The regression lines are fitted for each species and color-coded larch (red) and cembra pine (cyan). Pearson correlation coefficients (r) and *P*-values from the linear regressions are shown in each panel.

δ^2H-based pairs show little cross-species stability, whereas δ^{18}O–δ^{13}C yields a robust, scale-dependent coherence.

Climate sensitivities

We analyzed monthly correlations between mean raw isotope chronologies and climate variables over the whole observational period (1901–2015 CE), using temperature, precipitation, vapor pressure (VP), relative humidity (RH) and the Palmer Drought Severity Index (PDSI) (Figure 5). The results confirm that δ^{18}O exhibits the strongest and most consistent climate sensitivity across species, with constant positive correlations with temperature and negative correlations with hydroclimate indices, particularly during JJA. In contrast, δ^2H and δ^{13}C revealed species-specific patterns, with climate correlations generally strengthening when both species were combined for δ^{13}C (Figure 4).

The δ^{18}O values from both species showed consistent positive correlations with temperature and negative correlations with precipitation and PDSI, with the strongest relationships occurring during summer months (JJA). While precipitation correlations were generally below the significance threshold at the monthly scale, they became significant when aggregated at the seasonal level for both winter (DJF) and summer (JJA).

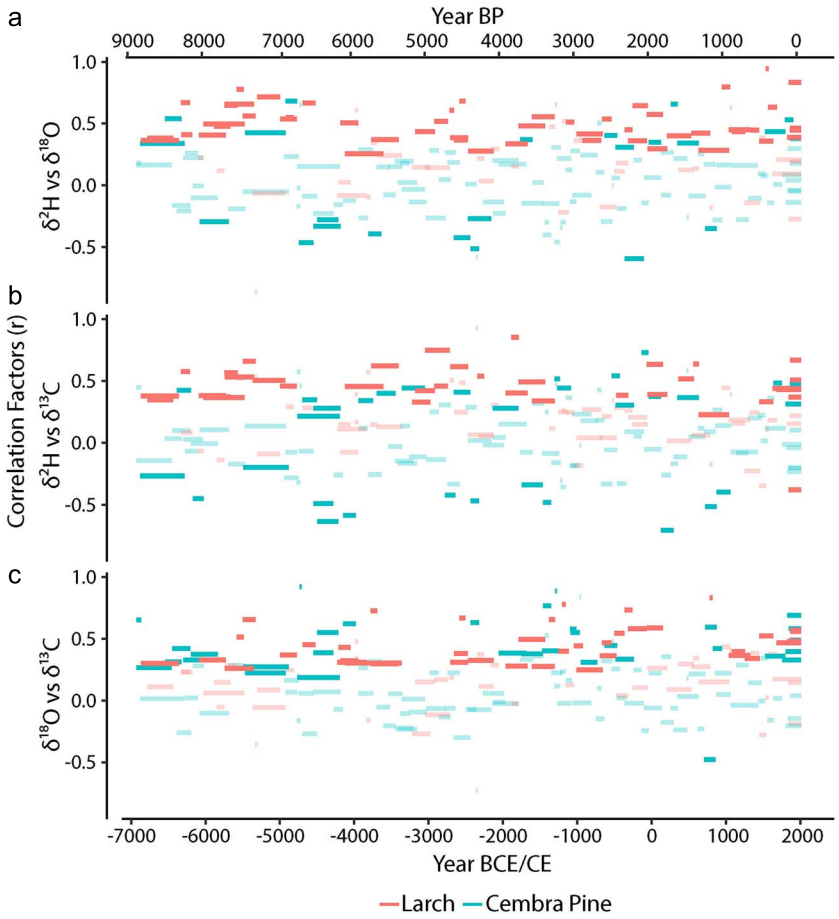

Figure 3. Temporal evolution of tree-level correlations among hydrogen (δ^2H), oxygen (δ^{18}O) and carbon (δ^{13}C) isotopic compositions of tree-ring cellulose. Pearson correlation coefficients (r) for δ^2H vs δ^{18}O (a), δ^2H vs δ^{13}C (b) and δ^{18}O vs δ^{13}C (c) are shown over time. Each segment represents an individual tree sample, with red for larch and cyan for cembra pine, with the length representing the tree's temporal span. Solid lines indicate significant correlations ($P < 0.05$), while transparent segments represent non-significant correlations.

These patterns were similar across species, and the correlation strength increased after merging the chronologies of both species.

The δ^2H–climate correlations displayed greater interspecies variability. The δ^2H values correlated positively with temperature in both species, though more weakly in cembra pine. In larch, but not cembra pine, δ^2H values showed strong negative correlations with PDSI, mirroring the pattern observed for δ^{18}O. Correlations between δ^2H and vapor pressure were generally positive but weaker than those observed for δ^{18}O.

The δ^{13}C–temperature correlations were positive for both species, with stronger values in larch, particularly in July and August. Precipitation correlations were negative during summer in both species, again more pronounced in larch. When the species were combined, the correlations to precipitation further increased. Larch showed negative correlations with PDSI throughout the growing season, while cembra pine showed a weak positive correlation with PDSI. Correlations with summer temperature and precipitation increased when species were merged; this was also confirmed in site-level analyses from the Engadin Valley (Figure S3 available as Supplementary Data at *Tree Physiology* Online), indicating that these patterns are not region-specific. First-differenced correlations (Figure S4 available as Supplementary Data at *Tree Physiology* Online) reveal similar seasonal patterns but with reduced magnitudes, indicating that long-term trends do not solely drive the observed relationships, but also reflect short-term variability. Alternative pairings such as δ^2H–VP/VPD can enhance the fit in certain seasonal windows. However, compared with δ^{13}C–precipitation they are less stable: at the site level the high-frequency signal is inconsistent (Figure S3 available as Supplementary Data at *Tree Physiology* Online), and the correlation weakens as the analysis window lengthens (Figure S4 available as Supplementary Data at *Tree Physiology* Online).

Further test merging δ^{18}O and δ^2H into a combined index does not improve the overall climate sensitivity beyond that already provided by δ^{18}O alone (Figure S5 available as Supplementary Data at *Tree Physiology* Online).

Climate sensitivity analysis reinforces the species coherence patterns shown earlier: δ^{18}O exhibits consistent interspecies agreement, while δ^2H and δ^{13}C are more variable, yet partially converge when aggregated. The isotope–climate responses thus confirm both the robustness of δ^{18}O and the physiological complexity of δ^2H and δ^{13}C.

Discussion

Species correlation

The analysis confirms strong and consistent relationships between larch and cembra pine δ^{18}O throughout both

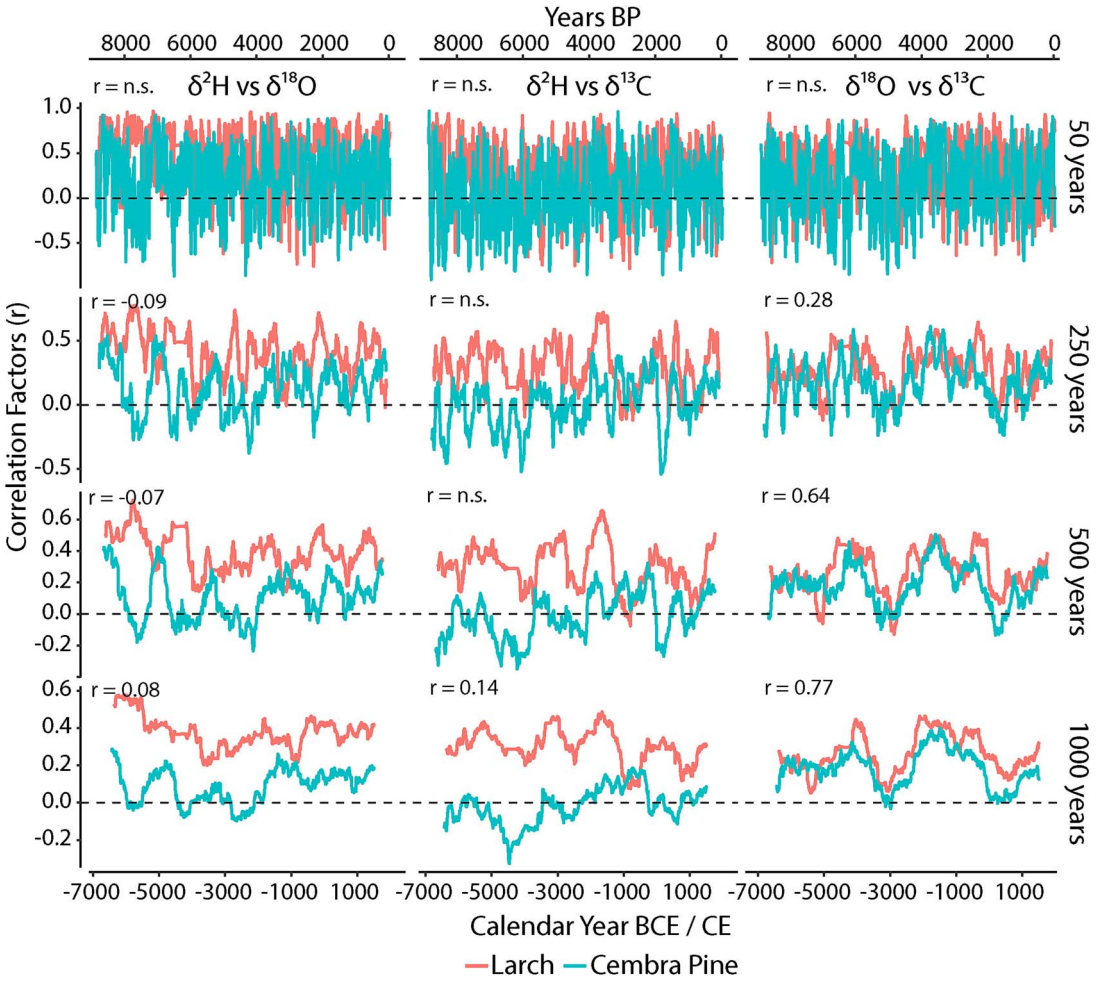

Figure 4. Temporal evolution of chronology-level correlations among hydrogen (δ^2H), oxygen (δ^{18}O) and carbon (δ^{13}C) isotopic compositions of tree-ring cellulose. Running Pearson correlations between isotope pairs (columns: δ^2H vs δ^{18}O, δ^2H vs δ^{13}C, δ^{18}O vs δ^{13}C) across four moving window lengths (columns: 50, 250, 500 and 1000 years). Correlations are shown separately for larch (red) and cembra pine (cyan). Labels at the top of each facet report the inter-species agreement of the running correlations; 'n.s.' denotes $P \geq 0.05$ (two-tailed).

Holocene and modern periods, regardless of sample replication (Figure 1). This confirms that δ^{18}O is dominated by environmental drivers rather than by species-specific physiology, in line with known spatial consistency (Saurer et al. 2012, Klesse et al. 2018, Treydte et al. 2024). Its stability across 9000 years underscores the long-term robustness of this signal for capturing large-scale hydroclimate variability, and in fact, δ^{18}O records have been thoroughly explored for paleoclimate applications (Büntgen et al. 2021, Yang et al. 2021, Nagavciuc et al. 2022, Arosio et al. 2025). The robust nature of δ^{18}O as a climate proxy stems from its direct link to source water and evaporative conditions (Klesse et al. 2018, Xu et al. 2024) and a relatively constant biochemical isotope fractionation (Roden et al. 2000), explaining its consistent patterns across diverse Alpine treeline locations (Saurer et al. 2012, Klesse et al. 2018, Balting et al. 2021, Field et al. 2022, Nagavciuc et al. 2023, Treydte et al. 2024). Important for this study, δ^{18}O stability across the two species provides a reference for interpreting the hydrogen and carbon isotope signals.

The δ^2H and δ^{13}C chronologies show interspecies divergence at both multi-millennial scales and in the modern period, despite different sample replications (Figure 1c–f). The divergence is attributed to species physiological processes, and not to the isotopic signals of source water for δ^2H and atmospheric CO_2 for δ^{13}C. Differences in rooting depth and water uptake patterns can be ruled out, since they would affect δ^{18}O, which is not observed. The variability of tree rings δ^2H may reflect differences in metabolic isotope fractionation (Cormier et al. 2018, Lehmann et al. 2024a). The evergreen cembra pine has a conservative growth strategy and extended carbon storage capacity. In contrast, the more opportunistic and fast-growing deciduous larch has the priority to rebuild its needles each spring by mobilizing carbohydrate stores (Carrer and Urbinati 2006, Rossi et al. 2009, Gruber et al. 2011), thus influencing seasonal isotopic inputs in tree rings (Peters et al. 2020). The weaker δ^2H–climate correlations of cembra pine agree with current knowledge of post-photosynthetic fractionation and remobilization processes in evergreens (Lehmann et al. 2021, Vitali et al. 2022, Charlet De Sauvage et al. 2025). Such weaker and more variable isotope-climate relationships are consistent with evidence that carbohydrate storage and carry-over processes can imprint strong non-climatic signals on tree physiological proxies, with isotope and anatomical records partly diverging due to internal carbon cycling (Römer et al. 2025) This strengthens our interpretation that cembra pine δ^2H, and to a lesser degree δ^{13}C, are strongly influenced by metabolic fractionations, in contrast to δ^{18}O, which

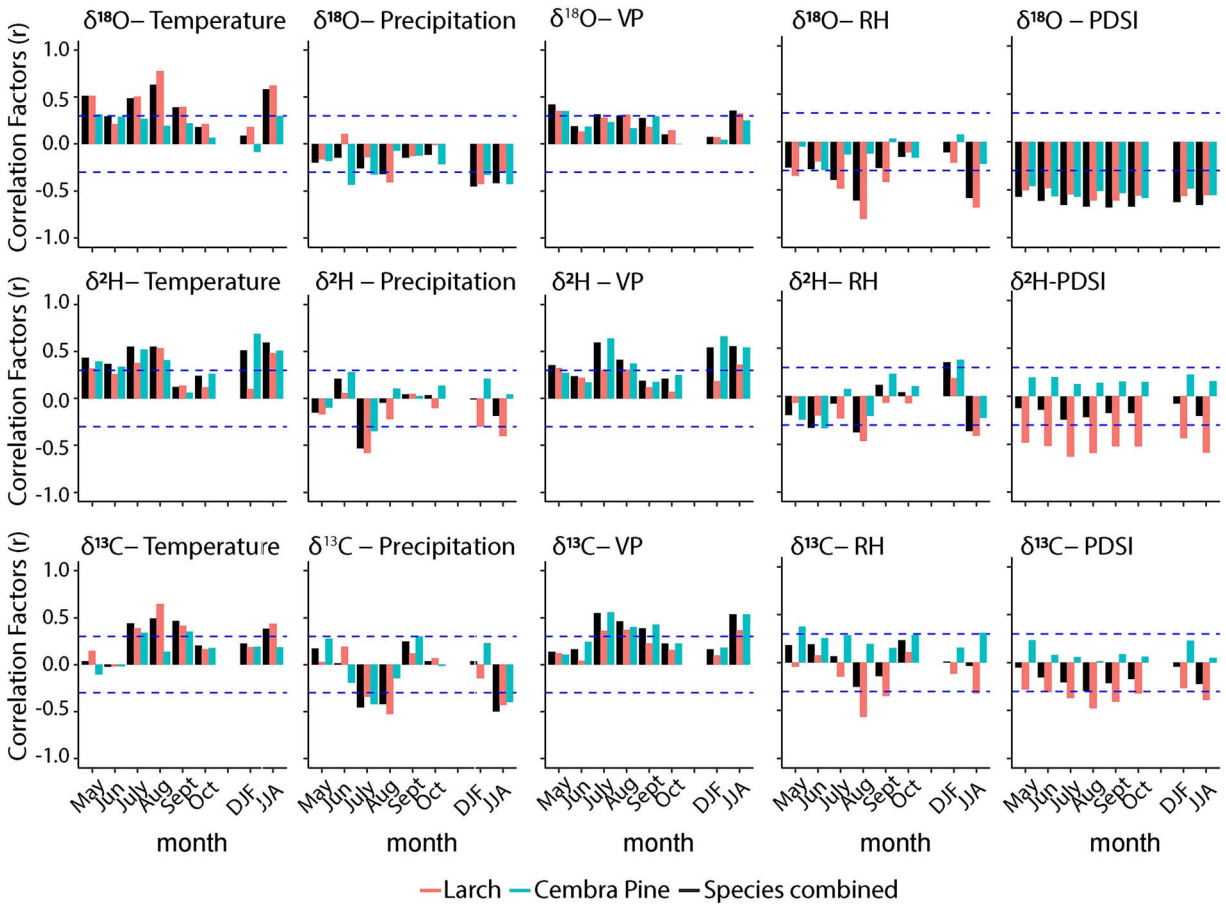

Figure 5. Monthly and seasonal correlations between stable isotope ratios of tree-ring cellulose and climate variables (1901–2015). Pearson correlation coefficients (*r*) between tree-ring δ^2H, δ^{18}O and δ^{13}C (row) and climate variables: Temperature, precipitation, vapor pressure (VP), relative humidity (RH) and the Palmer Drought Severity Index (PDSI). Climate variables are displayed monthly (may to October) and seasonal (winter—DJF and summer—JJA). Each panel represents a different isotope-climate relationship, with red bars representing larch and cyan bars representing cembra pine, black bars represent the two species combined. Dashed blue lines indicate the critical threshold of the Pearson correlation ($P < 0.05$).

remains primarily governed by environmental drivers. The species differences in δ^{13}C are in contradiction with previous results (Hartl-Meier et al. 2015) that were obtained from trees grown under temperate conditions, whereas our trees grown at treeline experienced harsher environmental stressors that may amplify physiological responses and affect δ^{13}C signals. Our findings show that species-specific physiology leaves a distinct imprint on δ^2H and δ^{13}C, contrasting with the species-independent environmental imprint on δ^{18}O. Replication statistics confirm that δ^{18}O is the most reliable signal (Table S1 available as Supplementary Data at *Tree Physiology* Online). Both larch and cembra pine exceed adequacy, and the pooled chronology is equally strong, underscoring the dominance of environmental control. δ^{13}C is close to the threshold, and δ^2H falls below, reflecting stronger species-specific physiology. Together, these contrasts highlight the robust climatic imprint on δ^{18}O and the physiological modulation of δ^{13}C, especially δ^2H.

The interspecies running correlations of δ^2H and δ^{13}C increase during the past ~200 years (Figure 1l). This trend may partly reflect improved common signal strength due to higher sample depth in the recent period (Figure 1h), but it could also indicate environmental forcing linked to recent climate change. Potential drivers include rising atmospheric CO_2 and associated fertilization effects, or other shifts in growing conditions. Importantly, the δ^{13}C values are corrected for the anthropogenic decline in atmospheric δ^{13}C, ensuring that the observed increase in coherence is not an artifact of changing source CO_2 but a physiological or environmental signal. As both sampling depth and environmental change coincide in the modern period, these two factors cannot be disentangled with certainty. By contrast, the absence of a comparable increase in δ^{18}O correlations over the past 200 years indicates that replication of two trees per species is already sufficient to maintain a stable common signal, and that further increases in sample depth do not lead to higher interspecies agreement. Our findings show that species-specific physiology leaves a distinct imprint on δ^2H and δ^{13}C, contrasting with the species-independent environmental imprint on δ^{18}O.

Inter-isotope relationships

The inter-isotope relationships offer valuable insight into the different physiological strategies of larch and cembra pine (Holloway-Phillips et al. 2023). The alignment of the δ^{13}C–δ^{18}O correlation across two species remains consistent over centennial to millennial timescales (Figures 2–4). This long-term co-variation indicates a dominant role of stomatal regulation for tree growth, e.g., during drought conditions, likely reflects shared hydroclimatic controls, primarily soil moisture availability and vapor pressure deficit

(Scheidegger et al. 2000, Roden and Farquhar 2012, Rodriguez-Caton et al. 2021, Siegwolf et al. 2023). The co-variation is notable despite the distinct mechanisms governing the two isotopes: $\delta^{13}C$ is primarily influenced by physiological processes, such as stomatal conductance and photosynthetic assimilation, while $\delta^{18}O$ is more strongly influenced by physical processes like evaporative enrichment during transpiration and source water dynamics. However, $\delta^{18}O$ also responds secondarily to stomatal behavior and source water variability (Siegwolf et al. 2023).

This observation aligns with the established dual-isotope framework, where synchronous increases in $\delta^{13}C$ and $\delta^{18}O$ reflect stomatal regulation under drought, while decoupling indicates shifts in photosynthetic capacity or reduced evaporative demand (Scheidegger et al. 2000, Siegwolf et al. 2023). This co-variance was observed before and has been used as a paleoclimate indicator, particularly for reconstructing drought conditions (Churakova et al. 2024). Across scales, the $\delta^{18}O$–$\delta^{13}C$ running correlations co-vary tightly between larch and pine, pointing to a shared environmental control on stomatal conductance and leaf-water enrichment, consistent with the dual-isotope framework (Siegwolf et al. 2023). Of interest, a marked decline in the strength of the $\delta^{13}C$–$\delta^{18}O$ correlation occurs around 5000 BP (Figures 3 and 4), coinciding with a humid phase in the central Alps (Arosio et al. 2025, Prochnow et al. 2025). This breakdown suggests that under conditions of reduced evaporative demand, the physiological link between $\delta^{13}C$ and $\delta^{18}O$ can weaken. This underscores a key limitation in applying dual-isotope interpretations uncritically across long temporal scales (Siegwolf et al. 2023).

The correlations involving hydrogen isotopes ($\delta^{2}H$–$\delta^{18}O$ and $\delta^{2}H$–$\delta^{13}C$) differ in the two species. In larch, the $\delta^{2}H$–$\delta^{18}O$ correlations are generally positive, consistent with previous findings (Hafner et al. 2011, Vitali et al. 2022) and likely reflect a shared climatic imprint mediated by precipitation (Dansgaard 1964) and evaporative enrichment of leaf water (Voelker et al. 2014). In this deciduous species, the needle development precedes or overlaps earlywood formation, creating a high early-season demand for reserves (Rossi et al. 2009, Kimak et al. 2015), therefore, the later growth may mostly rely on freshly assimilated carbohydrates. This may reduce metabolic effects on $\delta^{2}H$ and enhance the climatic imprint of the $\delta^{2}H$ of the complete tree ring. The apparent contradiction arising from the pronounced short-term $\delta^{2}H$–$\delta^{18}O$ decoupling observed during defoliation stress (Vitali et al. 2023) can be reconciled by the 5-year resolution of our data, which captures long-term variability and may smooth short-term responses. Cembra pine displays inconsistent, often both positive and negative $\delta^{2}H$–$\delta^{18}O$ correlations (Figures 2 and 3), aligning with previous observations in other evergreen conifers (Vitali et al. 2022, Charlet De Sauvage et al. 2025), and being potentially influenced by cambial age (Arosio et al. 2021). This suggests a stronger metabolic fingerprint in $\delta^{2}H$ that may vary from year to year depending on whether the climate is favorable for growth or not (Lehmann et al. 2022, Schmid and Schiffels 2023). While $\delta^{18}O$ is linked to leaf water signatures mediated by evaporative demand (Treydte et al. 2014, 2024), $\delta^{2}H$ is more affected by biological fractionations (Cormier et al. 2018) with patterns that vary between species. A weakening of $\delta^{2}H$–$\delta^{18}O$ coherence has been associated with increased use of stored carbohydrates and stronger changes in metabolic pathways under stress conditions (Vitali et al. 2024, Neycken et al. 2025).

Seasonal studies confirm that remobilization of starch and triose cycling can disrupt the expected positive $\delta^{2}H$–$\delta^{18}O$ relationship, producing decoupling in earlywood (Nabeshima et al. 2018). Such processes plausibly explain the negative $\delta^{2}H$–$\delta^{18}O$ correlations observed in some cembra pine individuals. One further possibility is that $\delta^{18}O$ and $\delta^{2}H$ are modulated by partly distinct physiological processes, which can drive divergent responses. Temperature-dependent isotope fractionation may act in opposite directions for oxygen and hydrogen (Schuler et al. 2025), and post-photosynthetic exchange (Pex) may vary between isotopes, occasionally producing negative $\delta^{18}O$–$\delta^{2}H$ relationships (Holloway-Phillips et al. 2023). In evergreens such as pine, the seasonality of reserve use and longer carbon-pool turnover should be considered when testing whether cellulose $\delta^{2}H$ remains primarily source-leaf driven, with similar implications for wood cellulose that can integrate prior-year assimilates (Holloway-Phillips et al., 2024). While most studies report Pex to be positively related across isotopes (Roden et al. 2000), our findings in pine suggest that flux-dependent metabolic routing and enzyme-level stereospecificity/kinetic isotope effects can decouple $\delta^{2}H$ from $\delta^{18}O$, consistent with recent frameworks that link $\delta^{2}H$ variation in carbohydrates to pathway fluxes and position-specific effects (Holloway-Phillips et al. 2024, 2025).

The $\delta^{2}H$–$\delta^{13}C$ relationship has been less explored in tree-ring studies, yet it provides additional insights into species-specific metabolism. In our data, significant positive correlations emerge in larch but not in pine (Figures 2–4). Rather than a strict 'fresh vs stored' tracer, we interpret $\delta^{2}H$–$\delta^{13}C$ as reflecting the joint sensitivity of C and H isotope fractionation to gas exchange and metabolic routing: stronger coupling in larch is consistent with steadier fluxes, whereas weaker/variable coupling in pine points to greater metabolic plasticity (e.g., variable storage use, pathway re-routing, and Pex differences) (Tcherkez et al. 2011, Cormier et al. 2019, Holloway-Phillips et al. 2024, Wieland et al. 2025). This interpretation follows the flux-proxy perspective for $\delta^{2}H$ in plant carbohydrates and the mechanistic role of NADPH-linked, stereospecific hydride transfers and KIEs in shaping whole-molecule $\delta^{2}H$ signals; experimental evidence in autotrophic tissues further links $\delta^{2}H$ to photosynthetic and metabolic fluxes (Cormier et al. 2019, Holloway-Phillips et al. 2024, Lehmann et al. 2024a). Taken together, we treat the $\delta^{2}H$–$\delta^{13}C$ link as a qualitative signal of how carbon is routed, not a strict on/off tracer. In larch, the stronger coupling fits rapid use of recent assimilates and relatively stable metabolic fluxes. In pine, the weaker and more variable coupling points to greater, and more flexible, use of stored substrates, with bigger shifts in metabolic routing under stress, which increases $\delta^{2}H$ variability for a given $\delta^{13}C$. A complementary view is that larch has lower metabolic acclimation (more constant pathways), whereas pine shows greater plasticity, which can decouple $\delta^{2}H$ from $\delta^{13}C$.

In contrast, the stable $\delta^{2}H$–$\delta^{18}O$ relationship in larch highlights its value as a reliable proxy for past moisture conditions. Our findings underscore the shared environmental imprint in $\delta^{18}O$ and the contrasting $\delta^{13}C$ and $\delta^{2}H$ isotope dynamics that reflect species-specific carbohydrate use and (post-)photosynthetic isotope fractionation processes.

Our results indicate that $\delta^{18}O$ in larch is strongly and consistently controlled by climate, with little evidence of physiological overprints. By contrast, pine $\delta^{18}O$ shows

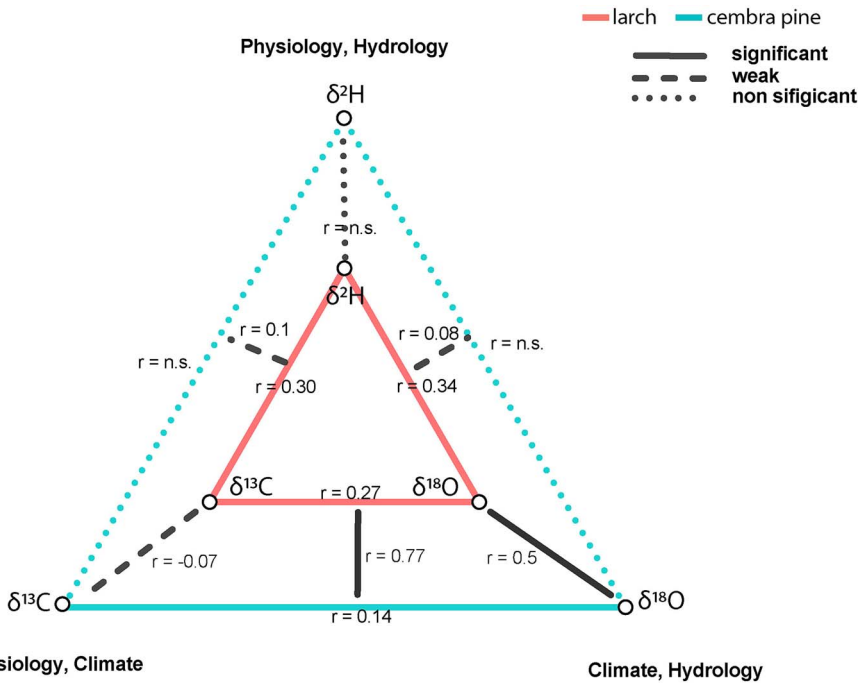

Figure 6. Schematic summary of inter-isotope relationships in larch (red) and cembra pine (blue). Line styles indicate significant (solid), weak (dashed) or non-significant (dotted) correlations. Correlation coefficients displayed are derived from three complementary analyses: Figure 1 (inter-species correlations), Figure 2 (intra-species correlations) and Figure 5 (temporal stability via running correlations). Larch shows consistently strong coupling among δ^2H, δ^{13}C and δ^{18}O, while pine displays weaker or inconsistent links, particularly involving δ^2H.

occasional negative correlations with δ^2H and weaker coherence with climate, suggesting that carbohydrate storage and post-photosynthetic fractionations can partly influence its isotopic composition. This interpretation is supported by (Nakatsuka et al. 2020), who demonstrated that metabolic effects can simultaneously alter δ^2H and δ^{18}O during cellulose synthesis on Japanese cypress. Thus, while δ^{18}O provides a robust hydroclimate signal across both species, it is particularly stable in larch, whereas pine δ^{18}O may carry a modest physiological imprint under conditions of enhanced storage use. These contrasting isotope linkages are summarized in a schematic synthesis (Figure 6), which highlights the strong triangular coupling among δ^2H, δ^{13}C and δ^{18}O in larch versus the weaker and more variable connections in cembra pine. This conceptual framework underlines that δ^{18}O is robustly climate-controlled, while δ^2H and δ^{13}C reflect species-specific physiological regulation. To help disentangle mechanisms, a parallel analysis of growth variability with the isotope series could clarify tree responses, following the δ^2H–growth covariation concept (Lehmann et al. 2021) and the shared links of δ^{13}C to photosynthesis and growth.

Climate sensitivity

The data show that δ^{18}O in both larch and cembra pine are correlated with summer conditions, positively with temperature and negatively with hydroclimate (RH and PDSI). Merging the values of the two species reinforces this seasonal signal (Figure 5). This shared climate sensitivity of δ^{18}O in the two species is consistent with previous multi-species comparisons (Grießinger et al. 2019), despite known differences in secondary growth responses (Obojes et al. 2022). However, some studies report that δ^{18}O in cembra pine in Carpathian and Alpine sites showed sensitivity to spring–summer humidity and precipitation (Nagavciuc et al. 2020, Lopez-Saez et al. 2024) and that δ^{18}O in larch in southeastern Alpine sites primarily responded to mid-late summer temperature and sunshine duration (Hafner et al. 2011). Our results do not indicate significant seasonality distinctions between species.

Across species, δ^{18}O tracks hydroclimate equally well in larch and pine, confirming a shared climatic control (Figure 4). The contrast appears in the H–O covariation: larch shows consistently positive δ^2H–δ^{18}O, whereas pine alternates between positive and negative correlations (Figure 3a). We interpret the negative cases as short-lived phases of heterotrophic dominance during wood formation, metabolic fractionations enrich δ^2H, while elevated oxygen exchange during cellulose synthesis depresses δ^{18}O, yielding a negative δ^2H–δ^{18}O correlations (Nabeshima et al. 2018, Martínez-Sancho et al. 2023).

Given the positive correlation between δ^{18}O and δ^2H, we tested whether combining δ^2H and δ^{18}O could enhance the climate signal by compensating for physiological noise (Figure S5 available as Supplementary Data at *Tree Physiology* Online). The combined index (δ^{18}O + δ^2H) yielded correlations broadly similar to those of δ^{18}O alone. These results confirm that δ^{18}O already provides the most stable and coherent hydroclimate proxy, while δ^2H adds complementary information on physiological processes rather than consistently strengthening the climate reconstruction potential.

The δ^2H values of the two species demonstrate a pronounced different climate sensitivity. Larch δ^2H displays a climate response similar to δ^{18}O, although somewhat weaker, confirming earlier findings from Slovenia and the ISONET dataset (Hafner et al. 2011, Vitali et al. 2022). Thus, larch δ^2H seems to be more linked to the composition of source and leaf water and less influenced by metabolic processes. On the other hand, cembra pine δ^2H shows no clear or

consistent climate signal, aligning with reports of δ^2H of other evergreen conifers that were more influenced by metabolic processes than by direct environmental drivers (Lehmann et al. 2022, Wieloch et al. 2022). The $\delta^{13}C$ in larch and cembra pine shows different sensitivity to summer hydroclimate, particularly to precipitation and vapor pressure, with larch having similar relationships but weaker than those of $\delta^{18}O$, as reported by Nagavciuc et al. (2020). However, for larch $\delta^{13}C$ in the Lötschental, a strong relationship with drought was observed (Kress et al. 2010) suggesting that $\delta^{13}C$–climate correlations can improve when sampling is restricted to smaller, climatically homogeneous regions, particularly in dry inner-Alpine valleys. Of interest, the strength of the precipitation climate signal increases by combining the $\delta^{13}C$ series of both species, suggesting that it emphasizes the shared environmental drivers. This increase in $\delta^{13}C$ under dry conditions likely reflects the effect of stomatal regulation, which reduces discrimination against ^{13}C during periods of water stress and results in higher $\delta^{13}C$ values (Farquhar et al. 1989).

The consistent coupling between δ^2H and $\delta^{18}O$ observed in larch but not in cembra pine likely reflects physiological differences in carbohydrate metabolism and allocation (Cormier et al. 2018). It suggests that in larch, the freshly assimilated carbohydrates are rapidly incorporated into cellulose with minimal isotopic modification, as supported by the high non-structural carbohydrate concentrations and tight phloem–xylem sugar coupling throughout the growing season (Gruber et al. 2013) that facilitates the direct transfer of environmental signals into cellulose (Cormier et al. 2019). In contrast, cembra pine exhibits weaker δ^2H–$\delta^{18}O$ coherence, indicative of greater metabolic fractionation linked to carbon storage and remobilization a physiological trait typical of evergreen conifers with year-round photosynthetic activity and asynchronous sink demands (Gruber et al. 2013, Cormier et al. 2018).

The $\delta^{13}C$–$\delta^{18}O$ coherence across species likely reflects reduced stomatal control under humid conditions, indicating that both isotopes are governed by climate-sensitive, rather than species-specific, stomatal regulation (Siegwolf et al. 2023).This matches the dual-isotope framework: positive C–O coupling arises when evaporative demand constrains g_s; under mesic conditions the coupling typically decreases (Saurer and Cherubini 2022, Siegwolf et al. 2023). Because C–O correlations are of comparable strength in both species, we infer that their A–g_s responses are similarly coordinated over the calibration period. This fits the DI model: $\delta^{18}O$ tracks evaporative enrichment and source water; $\delta^{13}C$ tracks ci/ca via stomatal regulation. Where C–O stays tight, climate dominates; where it decreases, physiology or humidity shifts become more visible (Siegwolf et al. 2023).

Conclusions

Altogether, larch reflects a more immediate, climate-synchronous growth mode, while cembra pine integrates carbon signals over longer timescales, modulated by storage, remobilization and possibly differential tissue allocation. These physiological differences are crucial for interpreting species-specific isotope signals and for designing robust, multi-species isotope-based climate reconstructions. Among the three isotopes, δ^2H shows the strongest species-specific differences and $\delta^{18}O$ the highest interspecies agreement, with $\delta^{13}C$ occupying an intermediate position. These findings underscore that δ^2H is not simply a duplicate of the $\delta^{18}O$ hydrological signal, but also encodes internal carbon metabolism and stress responses (Lehmann et al. 2021, Vitali et al. 2023).

Consequently, our data show that $\delta^{18}O$ is the most reliable climate proxy across species and timescales, outperforming $\delta^{13}C$ and δ^2H and supporting its use in long-term reconstruction. The climate precipitation sensitivity of $\delta^{13}C$ can be enhanced by integrating species records to reduce physiological noise, supporting multi-species $\delta^{13}C$ chronologies for hydroclimate reconstructions. The less directly climate-linked δ^2H provides insights into carbon-water interactions and internal plant functioning (Schuler et al. 2023), especially in evergreen species with asynchronous storage and growth dynamics. Its application as a direct paleoclimate proxy is limited, but it carries climatic and physiological signals that are valuable for interpreting stress responses and carbon allocation (Vitali et al. 2022, Charlet De Sauvage et al. 2025).

While $\delta^{18}O$ remains the most direct climate proxy, δ^2H and $\delta^{13}C$ provide additional insights into plant internal processes and drought responses, especially in evergreen species.

Our results demonstrate that inter-isotope links add information beyond single isotopes. In both species, $\delta^{13}C$–$\delta^{18}O$ behaves as a consistent proxy for climate-sensitive stomatal regulation. By contrast, δ^2H–$\delta^{18}O$ shows species-specific modulation, often weak/negative or variable in pine, but more coherent in larch. The δ^2H–$\delta^{13}C$ is strong in larch yet weak/variable in pine, indicating steadier fluxes in larch versus greater metabolic plasticity in pine. Together, these patterns provide a new physiological dimension to reconstructions using a multi-isotope approach, improving the separation of climate and species-specific physiology in long records.

Supplementary Data

Supplementary data for this article are available at *Tree Physiology* Online.

Author contributions

T.A. and M.S. designed the study. T.A. performed the statistical analyses. T.A. and M.S drafted the manuscript. All authors provided critical discussion, helped to write and revise the manuscript, and approved its submission.

Conflict of interest

The authors declare that they have no known competing financial interests or personal relationships that could have appeared to influence the work reported in this paper.

Funding

The study was supported by the Swiss National Science Foundation (SNSF; grant no. P5R5PN_225686, granted to T.A. and SNSF 200021L_144255, 200020_172550 granted to M.L.). M.M.L was supported by the SNSF (grant nos #213367 and #229377).

Data availability

The data used in this work are available on Pangaea http://dx.doi.org/10.1594/PANGAEA.941604.

References

Arosio T, Ziehmer-Wenz MM, Nicolussi K, Schlüchter C, Leuenberger M (2020) Larch cellulose shows significantly depleted hydrogen isotope values with respect to Evergreen conifers in contrast to oxygen and carbon isotopes. Front Earth Sci 8:579. https://doi.org/10.3389/feart.2020.523073.

Arosio T, Ziehmer-Wenz MM, Nicolussi K, Schlüchter C, Leuenberger MC (2021) Investigating masking effects of age trends on the correlations among tree ring proxies. Forests 12:1523.

Arosio T, Ziehmer M, Nicolussi K, Schluechter C, Thurner A, Östereicher A, Nyfeler P, Leuenberger MC (2022) Alpine Holocene triple tree ring isotope record. PANGAEA. https://doi.org/10.1594/PANGAEA.941604.

Arosio T, Büntgen U, Nicolussi K et al. (2024) Tree-ring δ 18O and δ 2H stable isotopes reflect the global meteoric water line. Front Earth Sci 12:1440064. https://doi.org/10.3389/feart.2024.1440064.

Arosio T, Leuenberger M, Nicolussi K et al. (2025) Tree-ring stable isotopes from the European Alps reveal long-term summer drying over the Holocene. Sci Adv 11:eadr4161. https://doi.org/10.1126/sciadv.adr4161.

Balting DF, Ionita M, Wegmann M et al. (2021) Large-scale climate signals of a European oxygen isotope network from tree rings. Clim Past 17:1005–1023.

Barbour MM (2007) Stable oxygen isotope composition of plant tissue: a review. Funct Plant Biol 34:83–94.

Boettger T, Haupt M, Knöller K et al. (2007) Wood cellulose preparation methods and mass spectrometric analyses of δ13C, δ18O, and nonexchangeable δ2H values in cellulose, sugar, and starch: an interlaboratory comparison. Anal Chem 79:4603–4612. https://doi.org/10.1021/ac0700023.

Borella S, Leuenberger M, Saurer M (1999) Analysis of δ18O in tree rings: wood-cellulose comparison and method dependent sensitivity. J Geophys Res Atmos 104:19267–19273. https://doi.org/10.1029/1999JD900298.

Briffa KR, Jones PD, Schweingruber FH, Karlén W, Shiyatov SG, (1996) Tree-ring variables as proxy-climate indicators: problems with low-frequency signals. In: Jones PD, Bradley RS, Jouzel J (eds), Climatic variations and forcing mechanisms of the last 2000 years. Springer Berlin Heidelberg, Berlin, Heidelberg, pp 9–41. https://doi.org/10.1007/978-3-642-61113-1_2

Büntgen U, Urban O, Krusic PJ et al. (2021) Recent European drought extremes beyond common era background variability. Nat Geosci 14:190–196. https://doi.org/10.1038/s41561-021-00698-0.

Carrer M, Urbinati C (2006) Long-term change in the sensitivity of tree-ring growth to climate forcing in *Larix decidua*. New Phytol 170: 861–872. https://doi.org/10.1111/j.1469-8137.2006.01703.x.

Charlet De Sauvage J, Saurer M, Treydte K, Lévesque M (2025) Decoupling of tree-ring cellulose δ^{18} O and δ^{2} H highlighted by their contrasting relationships to climate and tree intrinsic variables. Plant Cell Environ 48:1903–1918. https://doi.org/10.1111/pce.15252.

Churakova OV, Siegwolf RT, Zharkov MS, Saurer M (2024) Dual carbon and oxygen isotopes in Siberian tree rings as indicator of millennia sunshine duration changes. Sci Total Environ 927: 172042.

Coplen TB (1994) Reporting of stable hydrogen, carbon, and oxygen isotopic abundances (technical report). Pure Appl Chem 66: 273–276.

Cormier M-A, Werner RA, Sauer PE, Gröcke DR, Leuenberger MC, Wieloch T, Schleucher J, Kahmen A (2018) 2H-fractionations during the biosynthesis of carbohydrates and lipids imprint a metabolic signal on the δ2H values of plant organic compounds. New Phytol 218:479–491.

Cormier M-A, Werner RA, Leuenberger MC, Kahmen A (2019) 2 H-enrichment of cellulose and n-alkanes in heterotrophic plants. Oecologia 189:365–373.

Craig H (1954) Carbon 13 in plants and the relationships between carbon 13 and carbon 14 variations in nature. J Geol 62:115–149.

Dansgaard W (1964) Stable isotopes in precipitation. Tellus 16: 436–468.

Edvardsson J, Stoffel M, Corona C, Bragazza L, Leuschner HH, Charman DJ, Helama S (2016) Subfossil peatland trees as proxies for Holocene palaeohydrology and palaeoclimate. Earth Sci Rev 163: 118–140.

Esper J, Cook ER, Krusic PJ, Peters K, Schweingruber FH (2003) Tests of the RCS method for preserving low-frequency variability in long tree-ring chronologies. Tree Ring Res 59:81–98.

Farquhar GD, Sharkey TD (1982) Stomatal conductance and photosynthesis. Annu Rev Plant Physiol 33:317–345.

Farquhar GD, Ehleringer JR, Hubick KT (1989) Carbon isotope discrimination and photosynthesis. Annu Rev Plant Biol 40:503–537.

Field RD, Andreu-Hayles L, D'arrigo RD et al. (2022) Tree-ring cellulose δ18O records similar large-scale climate influences as precipitation δ18O in the Northwest Territories of Canada. Clim Dyn 58: 759–776. https://doi.org/10.1007/s00382-021-05932-4.

Filot MS, Leuenberger M, Pazdur A, Boettger T (2006) Rapid online equilibration method to determine the D/H ratios of non-exchangeable hydrogen in cellulose. Rapid Commun Mass Spectrom 20:3337–3344.

Friedrich M, Remmele S, Kromer B, Hofmann J, Spurk M, Kaiser KF, Orcel C, Küppers M (2004) The 12,460-year Hohenheim oak and pine tree-ring chronology from Central Europe—a unique annual record for radiocarbon calibration and paleoenvironment reconstructions. Radiocarbon 46:1111–1122.

Gessler A, Cailleret M, Joseph J et al. (2018) Drought induced tree mortality–a tree-ring isotope based conceptual model to assess mechanisms and predispositions. New Phytol 219:485–490.

Gessler A, Wieloch T, Saurer M, Lehmann MM, Werner RA, Kammerer B (2024) The marriage between stable isotope ecology and plant metabolomics – new perspectives for metabolic flux analysis and the interpretation of ecological archives. New Phytol 244:21–31. https://doi.org/10.1111/nph.19973.

Grießinger J, Bräuning A, Helle G, Schleser GH, Hochreuther P, Meier WJ-H, Zhu H (2019) A dual stable isotope approach unravels common climate signals and species-specific responses to environmental change stored in multi-century tree-ring series from the Tibetan plateau. Geosciences 9:151.

Gruber A, Pirkebner D, Oberhuber W, Wieser G (2011) Spatial and seasonal variations in mobile carbohydrates in *Pinus cembra* in the timberline ecotone of the central Austrian Alps. Eur J For Res 130: 173–179.

Gruber A, Pirkebner D, Oberhuber W (2013) Seasonal dynamics of mobile carbohydrate pools in phloem and xylem of two alpine timberline conifers. Tree Physiol 33:1076–1083.

Hafner P, Robertson I, McCarroll D et al. (2011) Climate signals in the ring widths and stable carbon, hydrogen and oxygen isotopic composition of *Larix decidua* growing at the forest limit in the southeastern European Alps. Trees 25:1141–1154.

Harris I, Osborn TJ, Jones P, Lister D (2020) Version 4 of the CRU TS monthly high-resolution gridded multivariate climate dataset. Sci Data 7:109.

Hartl-Meier C, Zang C, Büntgen ULF, Esper JAN, Rothe A, Göttlein A, Dirnböck T, Treydte K (2015) Uniform climate sensitivity in tree-ring stable isotopes across species and sites in a mid-latitude temperate forest. Tree Physiol 35:4–15.

Helama S, Arppe L, Timonen M, Mielikäinen K, Oinonen M (2018) A 7.5 ka chronology of stable carbon isotopes from tree rings with implications for their use in palaeo-cloud reconstruction. Glob Planet Change 170:20–33. https://doi.org/10.1016/j.gloplacha.2018.08.002.

Holloway-Phillips M, Cernusak LA, Nelson DB, Lehmann MM, Tcherkez G, Kahmen A (2023) Covariation between oxygen and hydrogen stable isotopes declines along the path from xylem water to wood cellulose across an aridity gradient. New Phytol 240: 1758–1773. https://doi.org/10.1111/nph.19248.

Holloway-Phillips M, Tcherkez G, Wieloch T, Lehmann MM, Werner RA (2024) Is photosynthesis-derived NADPH really a source of 2 H-depleted hydrogen in plant compounds? Plant Cell Environ 48:4083–4098. https://doi.org/10.1111/pce.15403

Huang R, Xu C, Grießinger J, Feng X, Zhu H, Bräuning A (2024) Rising utilization of stable isotopes in tree rings for climate change and forest ecology. J For Res 35:13. https://doi.org/10.1007/s11676-023-01668-5.

Kimak A, Kern Z, Leuenberger M (2015) Qualitative distinction of autotrophic and heterotrophic processes at the leaf level by means of triple stable isotope (C–O–H) patterns. Front Plant Sci 6:1008.

Klesse S, Weigt R, Treydte K, Saurer M, Schmid L, Siegwolf RT, Frank DC (2018) Oxygen isotopes in tree rings are less sensitive to changes in tree size and relative canopy position than carbon isotopes. Plant Cell Environ 41:2899–2914.

Kress A, Saurer M, Siegwolf RT, Frank DC, Esper J, Bugmann H (2010) A 350 year drought reconstruction from Alpine tree ring stable isotopes. Global Biogeochemical Cycles, 24. https://doi.org/10.1029/2009GB003613

Lehmann MM, Vitali V, Schuler P, Leuenberger M, Saurer M (2021) More than climate: hydrogen isotope ratios in tree rings as novel plant physiological indicator for stress conditions. Dendrochronologia 65:125788.

Lehmann MM, Schuler P, Cormier M-A, Allen ST, Leuenberger M, Voelker S (2022) The stable hydrogen isotopic signature: From source water to tree rings. In Siegwolf RTW, Renée Brooks J, Roden J, Saurer M. (Eds.), Stable isotopes in tree rings: Inferring physiological, climatic and environmental responses (Tree Physiology, Vol. 8, pp. 331–359). Cham, Switzerland: Springer International Publishing. https://doi.org/10.1007/978-3-030-92698-4_11

Lehmann MM, Diao H, Ouyang S, Gessler A (2024*a*) Different responses of oxygen and hydrogen isotopes in leaf and tree-ring organic matter to lethal soil drought. Tree Physiol 44:tpae043.

Lehmann MM, Schuler P, Werner RA, Saurer M, Wiesenberg GLB, Cormier M-A (2024*b*) Biochemical and biophysical drivers of the hydrogen isotopic composition of carbohydrates and acetogenic lipids. Sci Adv 10:eadl3591. https://doi.org/10.1126/sciadv.adl3591.

Leuenberger M (2007) To what extent can ice core data contribute to the understanding of plant ecological developments of the past? Terr Ecol 1:211–233.

Leuenberger MC, Filot MS (2007) Temperature dependencies of high-temperature reduction on conversion products and their isotopic signatures. Rapid Comm Mass Spectrom 21:1587–1598. https://doi.org/10.1002/rcm.2998.

Liu Y, Song H, An Z et al. (2025) Recent centennial drought on the Tibetan plateau is outstanding within the past 3500 years. Nat Commun 16:1–9. https://doi.org/10.1038/s41467-025-56687-z.

Loader NJ, Santillo PM, Woodman-Ralph JP et al. (2008) Multiple stable isotopes from oak trees in southwestern Scotland and the potential for stable isotope dendroclimatology in maritime climatic regions. Chem Geol 252:62–71.

Loader NJ, Street-Perrott FA, Daley TJ et al. (2015) Simultaneous determination of stable carbon, oxygen, and hydrogen isotopes in cellulose. Anal Chem 87:376–380.

Lopez-Saez J, Corona C, Slamova L, Huss M, Daux V, Nicolussi K, Stoffel M (2024) Multiproxy tree ring reconstruction of glacier mass balance: insights from *Pinus cembra* trees growing near Silvretta glacier (Swiss Alps). Clim Past 20:1251–1267.

Martínez-Sancho E, Cernusak LA, Fonti P et al. (2023) Unenriched xylem water contribution during cellulose synthesis influenced by atmospheric demand governs the intra-annual tree-ring δ^{18}O signature. New Phytol 240:1743–1757. https://doi.org/10.1111/nph.19278.

McCarroll D, Loader NJ (2004) Stable isotopes in tree rings. Quaternary Sci Rev 23:771–801. https://doi.org/10.1016/j.quascirev.2003.06.017.

Nabeshima E, Nakatsuka T, Kagawa A, Hiura T, Funada R (2018) Seasonal changes of δD and δ18O in tree-ring cellulose of *Quercus crispula* suggest a change in post-photosynthetic processes during earlywood growth. Tree Physiol 38:1829–1840.

Nagavciuc V, Michel SL, Balting DF, Helle G, Freund M, Schleser GH, Steger DN, Lohmann G, Ionita M (2023) A past and present perspective on the European summer vapour pressure deficit. Clim Past Discuss 2023:1–29.

Nagavciuc V, Kern Z, Ionita M, Hartl C, Konter O, Esper J, Popa I (2020) Climate signals in carbon and oxygen isotope ratios of Pinus cembra tree-ring cellulose from the Călimani Mountains, Romania. Int J Climatol 40:2539–2556.

Nagavciuc V, Ionita M, Kern Z, McCarroll D, Popa I (2022) A ~700 years perspective on the 21st century drying in the eastern part of Europe based on δ18O in tree ring cellulose. Commun Earth Environ 3:277. https://doi.org/10.1038/s43247-022-00605-4.

Nakatsuka T, Sano M, Li Z et al. (2020) A 2600-year summer climate reconstruction in Central Japan by integrating tree-ring stable oxygen and hydrogen isotopes. Clim Past 16:2153–2172. https://doi.org/10.5194/cp-16-2153-2020,%25202020.

Neycken A, Lehmann MM, Saurer M, Wohlgemuth T, Frei ER, Lévesque M (2025) Understanding physiological mechanisms of European beech dieback responses to climate using a triple isotope approach in northern Switzerland. Dendrochronologia 91:126335.

Nicolussi K, Kaufmann M, Melvin TM, Van Der Plicht J, Schießling P, Thurner A (2009) A 9111 year long conifer tree-ring chronology for the European Alps: a base for environmental and climatic investigations. Holocene 19:909–920. https://doi.org/10.1177/0959683609336.

Obojes N, Meurer AK, Newesely C, Tasser E, Oberhuber W, Mayr S, Tappeiner U (2022) Swiss stone pine growth benefits less from recent warming than European larch at a dry-inner alpine forest line as it reacts more sensitive to humidity. Agric For Meteorol 315:108788.

Peters RL, Miranda JC, Schönbeck L et al. (2020) Tree physiological monitoring of the 2018 larch budmoth outbreak: preference for leaf recovery and carbon storage over stem wood formation in *Larix decidua*. Tree Physiol 40:1697–1711.

Prochnow M, Danius L, Strobel P, Rey F, Rittmeier L, Zech M, Tinner W, Zech R (2025) Wetter or drier? Paleohydrological evidence from a 30-year resolution Holocene biomarker δD record from Moossee. Switzerland Quaternary Sci Rev 369:109602.

Qi X, Treydte K, Saurer M et al. (2024) Contrasting water-use strategies to climate warming in white birch and larch in a boreal permafrost region. Tree Physiol 44:tpae053.

Rezzouk FZ, Serret MD, Araus JL, Bragado RS (2025) δ2H, δ18O, and δ13C behave differently when assessing transpirative and photosynthetic performance of wheat under contrasting VPD conditions. Crop 13:J1093–1105.

Roden JS, Farquhar GD (2012) A controlled test of the dual-isotope approach for the interpretation of stable carbon and oxygen isotope ratio variation in tree rings. Tree Physiol 32:490–503.

Roden JS, Lin G, Ehleringer JR (2000) A mechanistic model for interpretation of hydrogen and oxygen isotope ratios in tree-ring cellulose. Geochim Cosmochim Acta 64:21–35.

Rodriguez-Caton M, Andreu-Hayles L, Morales MS et al. (2021) Different climate sensitivity for radial growth, but uniform for tree-ring stable isotopes along an aridity gradient in *Polylepis tarapacana*, the world's highest elevation tree species. Tree Physiol 41:1353–1371.

Römer P, Wieland A, Torbenson MC et al. (2025) Covariance and climate signals among state-of-the-art tree-ring proxies. Quat Sci Rev 355:109270.

Rossi S, Rathgeber CB, Deslauriers A (2009) Comparing needle and shoot phenology with xylem development on three conifer species in Italy. Ann For Sci 66:1–8.

Rozanski K, Araguás-Araguás L, Gonfiantini R (1992) Relation between long-term trends of Oxygen-18 isotope composition of precipitation and climate. Science 258:981–985. https://doi.org/10.1126/science.258.5084.981.

Sanchez-Bragado R, Serret MD, Marimon RM, Bort J, Araus JL (2019) The hydrogen isotope composition δ2H reflects plant performance. Plant Physiol 180:793–812.

Saurer M, Cherubini P (2022) Tree physiological responses after biotic and abiotic disturbances revealed by a dual isotope approach. Tree Physiol 42:1–4.

Saurer M, Siegenthaler U, Schweingruber F (1995) The climate-carbon isotope relationship in tree rings and the significance of site conditions. Tellus B 47:320–330.

Saurer M, Kress A, Leuenberger M, Rinne KT, Treydte KS, Siegwolf RT (2012) Influence of atmospheric circulation patterns on the oxygen isotope ratio of tree rings in the Alpine region. J Geophys Res Atmos 117:D5.

Saurer M, Oettli M, Lehmann MM (2025) A simple method for triple stable isotope analysis of cellulose, sugar, and bulk organic matter—advances and limitations. Rapid Comm Mass Spectrom 39:e9957. https://doi.org/10.1002/rcm.9957.

Scheidegger Y, Saurer M, Bahn M, Siegwolf R (2000) Linking stable oxygen and carbon isotopes with stomatal conductance and photosynthetic capacity: a conceptual model. Oecologia 125:350–357. https://doi.org/10.1007/s004420000466.

Schmid C, Schiffels S (2023) Estimating human mobility in Holocene Western Eurasia with large-scale ancient genomic data. Proc Natl Acad Sci U S A 120:e2218375120. https://doi.org/10.1073/pnas.2218375120.

Schuler P, Vitali V, Saurer M, Gessler A, Buchmann N, Lehmann MM (2023) Hydrogen isotope fractionation in carbohydrates of leaves and xylem tissues follows distinct phylogenetic patterns: a common garden experiment with 73 tree and shrub species. New Phytol 239: 547–561. https://doi.org/10.1111/nph.18976.

Schuler P, Didion-Gency M, Vitali V, Saurer M, Oettli M, Diao H, Buchmann N, Gessler A, Lehmann MM (2025) Hot and hungry-high temperatures induce changes in leaf carbon dynamics and sugar isotope fingerprints. NPJ Sci Plants 1:12.

Sidorova OV, Siegwolf RT, Saurer M, Naurzbaev MM, Vaganov EA (2008) Isotopic composition (δ13C, δ18O) in wood and cellulose of Siberian larch trees for early medieval and recent periods. Geophys Res Biogeosci 113:G2.

Siegwolf RT, Brooks JR, Roden J, Saurer M (2022) Stable isotopes in tree rings: Inferring physiological, climatic and environmental responses., (p. 773). Springer Nature.

Siegwolf RTW, Lehmann MM, Goldsmith GR, Churakova (Sidorova OV, Mirande-Ney C, Timoveeva G, Weigt RB, Saurer M (2023) Updating the dual C and O isotope—gas-exchange model: a concept to understand plant responses to the environment and its implications for tree rings. Plant Cell Environ 46:2606–2627. https://doi.org/10.1111/pce.14630.

Tcherkez G, Mahé A, Hodges M (2011) 12C/13C fractionations in plant primary metabolism. Trends Plant Sci 16:499–506.

Treydte K, Boda S, Graf Pannatier E et al. (2014) Seasonal transfer of oxygen isotopes from precipitation and soil to the tree ring: source water versus needle water enrichment. New Phytol 202: 772–783.

Treydte K, Liu L, Padrón RS et al. (2024) Recent human-induced atmospheric drying across Europe unprecedented in the last 400 years. Nat Geosci 17:58–65.

Treydte KS, Schleser GH, Helle G, Frank DC, Winiger M, Haug GH, Esper J (2006) The twentieth century was the wettest period in northern Pakistan over the past millennium. Nature 440: 1179–1182. https://doi.org/10.1038/nature04743.

Vitali V, Martínez-Sancho E, Treydte K et al. (2022) The unknown third–hydrogen isotopes in tree-ring cellulose across Europe. Sci Total Environ 813:152281.

Vitali V, Peters RL, Lehmann MM, Leuenberger M, Treydte K, Büntgen U, Schuler P, Saurer M (2023) Tree-ring isotopes from the Swiss Alps reveal non-climatic fingerprints of cyclic insect population outbreaks over the past 700 years. Tree Physiol 43: 706–721.

Vitali V, Schuler P, Holloway-Phillips M et al. (2024) Finding balance: tree-ring isotopes differentiate between acclimation and stress-induced imbalance in a long-term irrigation experiment. Glob Chang Biol 30:e17237. https://doi.org/10.1111/gcb.17237.

Voelker SL, Brooks JR, Meinzer FC et al. (2014) Reconstructing relative humidity from plant δ18O and δD as deuterium deviations from the global meteoric water line. Ecol Appl 24:960–975.

Wieland A, Schuler P, Saurer M, Vitali V, Greule M, Keppler F, Lehmann MM (2025) Dual isotope analysis reveals phylogenetic patterns and novel insights into methoxy group synthesis of structural biomolecules in leaf and woody plant tissues. Plant Cell Environ 48:8483–8501. https://doi.org/10.1111/pce.70134.

Wieloch T, Grabner M, Augusti A, Serk H, Ehlers I, Yu J, Schleucher J (2022) Metabolism is a major driver of hydrogen isotope fractionation recorded in tree-ring glucose of *Pinus nigra*. New Phytol 234: 449–461. https://doi.org/10.1111/nph.18014.

Xu C, Huang R, An W, Zhao Q, Zhao Y, Ren J, Liu Y, Guo Z (2024) Tree ring oxygen isotope in Asia. Glob Planet Change 232:104348.

Yang B, Qin C, Bräuning A et al. (2021) Long-term decrease in Asian monsoon rainfall and abrupt climate change events over the past 6,700 years. Proc Natl Acad Sci USA 118:e210200 7118.

Zeileis A, Grothendieck G, Ryan JA, Andrews F, Zeileis MA (2014) Package 'zoo'. R Package Version 1–7. https://cran.r-project.org/web/packages/zoo/index.html

Ziehmer MM, Nicolussi K, Schlüchter C, Leuenberger M (2018) Preliminary evaluation of the potential of tree-ring cellulose content as a novel supplementary proxy in dendroclimatology. Biogeosciences 15:1047–1064. https://doi.org/10.5194/bg-15-1047-2018,%25202018.

Tree Physiology, 2026, 46, tpaf166
https://doi.org/10.1093/treephys/tpaf166
Research paper